BACHELOR

Rotating cluster assay

dose response and angular dependence of light scattering

Geraerts, R.W.L.

Award date:
2014

Rotating cluster assay: dose response and angular dependence of light scattering

R.W.L. Geraerts
MBx 2014-01

Supervisors:

R.W.L. van Vliembergen, MSc

Dr. L.J. van IJzendoorn

Molecular Biosensors for Medical Diagnostics

Department of Applied Physics

Eindhoven University of Technology

Abstract

One biosensor concept, is a so-called rotating cluster assay. The target molecules are sandwiched between superparamagnetic beads using so-called magnetic chaining, in which a pulsating magnetic field is used to bring the beads together much faster. After this magnetic chaining step, a rotating magnetic field is applied to the assay, and the formed chains start rotating. By focusing a laser beam on a small volume inside the sample and measuring the amount of scattered light, a measure for the amount of chains is obtained. This amount can be used to deduce the concentration of target molecules.

In this project, research is done on optimization of an assay which can be used, and the settings of the magnetic field in the chaining step. When there is no target present in the assay, ideally, there would be no clusters of particles at all. In practice, however, there will be non-specific clusters formed. Various parameters are varied to keep the amount of non-specific clusters as low as possible, without completely suppressing the formation of the wanted, specific bonds. With the optimized assay, a dose response curve is made. Also, the formed clusters are examined using a microscope, and the angular dependence of the light scattering is examined.

It turns out that the assay which works best, consists of phosphate buffered saline (PBS) as a buffer fluid, containing 1% bovine serum albumin (BSA), 0.5% Tween® 20 and 0.1 mg/ml superparamagnetic beads. The amplitude of the magnetic field used for the magnetic chaining is 11.4 mT. From the measured dose response curve, it follows that it is possible to reliably detect target concentrations between 5 and 50 pM. Also, the clusters are observed using a microscope, after the assay went through the chaining step. It is found that the amount of doublets and larger clusters indeed grows as a function of the target concentration, which matches the preceding expectations and experimental results.

The last part of this project involved measuring the angular dependence of the light scattering of the clusters. It turns out that the shape of the photodiode signal depends on the scattering angle. When the angle of the photodiode is increased from 60 to 130 degrees, a change can be seen in the number of small peaks per main peak of the signal. At first, only one peak is present, at 90 degrees there are clearly three visible peaks, and at 97 degrees even five peaks are observed. These peak disappear again if the angle is increased even more. At angles around 90 degrees, the total amount of detected light is low, but the higher frequency components of the Fourier transform of the photodiode signal play a more significant role than at small angles. When the angle is increased even more, the total amount of detected light increases again. This is the result of light scattered in a forward direction, but reflected by the glass cuvette in a backward direction.

Table of contents

1. Introduction

As the name indicates, the group *Molecular Biosensors for Medical Diagnostics* (MBx) at Eindhoven University of Technology (TU/e), focuses on research involving biosensors. A biosensor is a device used to detect the concentration of a biomarker, typically in a bodily fluid. Biomarkers are small molecules, like proteins, antibodies, DNA or RNA molecules, for which their concentration in a bodily fluid is indicative of a certain disease. A well-known example of a biosensor, pictured in figure 1, is the device diabetes patients use to measure their blood glucose levels. In the upcoming decades, these devices will be of great importance, as 4.4% of the entire human population will suffer from diabetes in 2030 [1]. Other biomarkers, however, may be found in concentrations that are more than a million times lower than the typical concentration of blood glucose [2]. Because there are so many different biomarkers with different properties, occurring in different concentrations, a wide variety exists in the concepts that are used in biosensors.

Figure 1: A blood glucose meter (OneTouch® UltraMini®), is a common example of a biosensor [3].

One of these concepts, is a so-called rotating cluster assay. The target molecules are sandwiched between superparamagnetic beads using so-called magnetic chaining [4][5], in which a pulsating magnetic field is used to bring the beads together much faster. In this way, the probability of forming bonds between beads and target molecules is enhanced. The off-time of the pulsating field is much longer than the on-time, to give the beads the time to move away from each other due to random motion [6]. During this off-time, the weaker bonds between two beads without a target molecule between them, that are also formed due to the magnetic field, are broken. After this magnetic chaining step, a rotating magnetic field is applied to the assay, and the formed chains start rotating. By focusing a laser beam on a small volume inside the sample and measuring the amount of scattered light, a measure for the amount of chains is obtained. This amount can be used to deduce the concentration of target molecules.

In this project, research is done on optimization of an assay which can be used, and the settings of the magnetic field in the chaining step. When there is no target present in the assay, ideally, there would be no clusters of particles at all. In practice, however, there will be non-specific clusters formed. Non-specific clusters consist of magnetic beads that stick together without target molecules between them. Various parameters are varied to keep the amount of non-specific clusters as low as possible, without completely suppressing the formation of the wanted, specific bonds. With the optimized assay, a dose response curve is made. Also, the formed clusters are examined using a microscope, and the angular dependence of the light scattering is examined.

First, in chapter 2, the theoretical background behind all conducted experiments is presented. The process of cluster formation due to magnetic chaining, and the processing of the signals are explained. Chapter 3 gives an overview of the way in which the experiments are preformed, the reason for these experiments, and the materials that are used. In chapter 4, the results of all of these experiments are presented, and these are compared to the results that are expected.

2. Theory

2.1 Assay

An immunoassay is a test which is used to detect specific molecules, or to measure the concentration of these target molecules. The three general components that are present in the assay used in this project are the buffer fluid, the target molecules and superparamagnetic beads. The beads are coated with antibodies, which have a very high affinity for the molecular composition of the target molecules. Specific concentrations of various other components can be added to the immunoassay, in an attempt to enhance the ratio between specific and non-specific clusters.

2.2 Superparamagnetic particles

The particles that are used are superparamagnetic, which means that they consist of different magnetic domains. Without an external magnetic field, these domains are all magnetized in a random direction depending on shape, surface and crystalline anisotropy. Under the influence of temperature, this magnetization can randomly change its orientation, but on average the magnetization of each particle is zero. When an external magnetic field is applied, the magnetizations of the domains will align in the direction of this field, and the material becomes magnetized. When the field is turned off again, the particles lose their magnetic properties. These properties of the particles are used in magnetic chaining.

2.3 Cluster formation

Clusters of particles can be formed when these particles are close enough to each other. If the only action bringing the particles closer together is random movement, it will take a lot of time before a sufficient amount of clusters is formed. To speed up this process, magnetic chaining is used. In the chaining step, a pulsating magnetic field is applied to the assay, which aligns the magnetic particles when it is turned on. When the field is turned off again, the particles will diffuse due to Brownian motion. Most of the non-specific bonds will break, and the stronger specific bonds between beads and target molecules will remain. To allow the non-specific bond to break, the off-time of the magnetic field is longer than the on-time. This is because Brownian motion is a much slower process than the motion of the particles due to the magnetic force. How long the off-time should be with respect to the on-time, is determined by A. Ranzoni [6]. This is done by optimizing the optical scattering signal due to binding of the particles as a function of the off-time of the field. The principle of magnetic chaining is visualized in figure 2.

When the concentration of the target molecule is low, most of the formed clusters will consist of two magnetic particles sandwiching one target molecule. When the target concentration is increased, less single particles will be left, and bigger clusters, like triples, will be formed. Besides target concentration, there are a lot more factors which together determine the number and type of clusters. Examples are the concentration of the beads, the amplitude of the magnetic field in the chaining step, and the concentrations of specific chemicals which have the ability to block some of the binding sites on the beads.

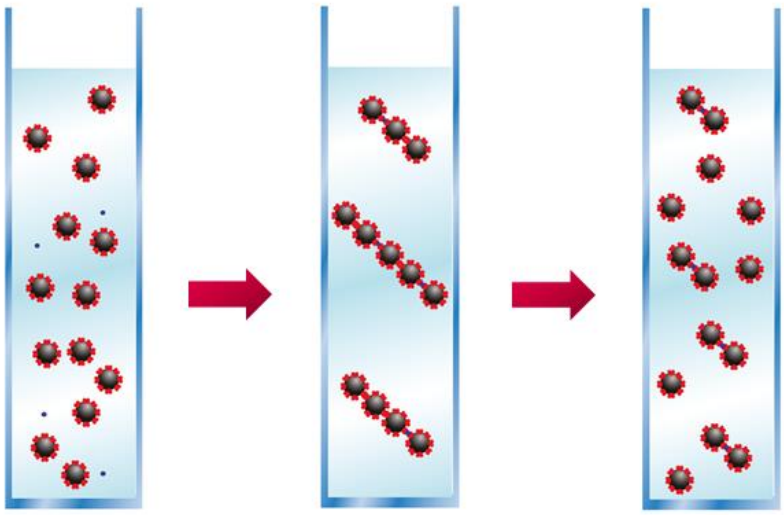

Figure 2: Schematic representation of the magnetic chaining process. The small dots are the target molecules, and the big grey ones are the coated superparamagnetic beads. In the left cuvette, the particles are randomly moving through the fluid. In the middle cuvette, a magnetic field is applied which aligns the particles. In the right cuvette, the field is turned off again, and only the non-specific bonds are broken. This process is repeated a couple of times.

2.4 Detection

By applying a rotating magnetic field, the formed clusters will start to rotate. Rotating chains in a fluid experience viscous drag. When the magnetic force and the viscous drag acting on the chains is in equilibrium, the chains will rotate at a constant velocity. At a certain angular frequency of the magnetic field, however, due to the viscous drag, the chains cannot keep up with the rotation of the field anymore. This frequency is called the critical frequency. Above the critical frequency, a growing phase lag arises between the direction of the magnetic field and the axis of the chain of beads. When this phase lag grows larger than 90 degrees, the chain starts rotating the other way around, and the chains will start moving in a wiggling motion pattern. See figure 3. The magnetic torque acting on a chain of beads is a function of the length of the chain, while the viscous drag acting on it, is a function of the square of the length of the chain. For longer chains, drag forces will overcome the magnetic torque, which is the reason why the critical frequency is lower for bigger clusters. The mathematical background for this phenomenon is provided by J.M. van Kemenade [2] and A. Ranzoni [6].

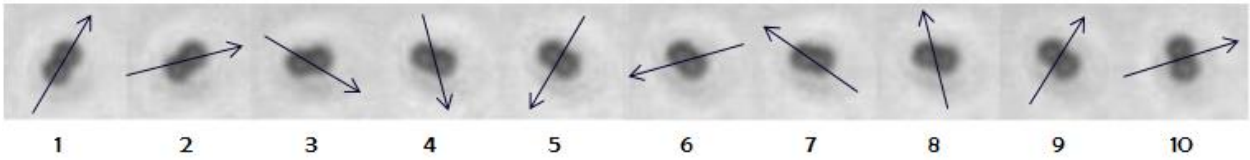

Figure 3: The wiggling motion of a doublet. The arrows indicate the direction of the magnetic field. The phase lag of the rotating cluster is ninety degrees between the fifth and sixth picture. At this point, the doublet starts rotating the other way around.

Due to the rotation of the clusters, their scattering area will oscillate as a function of time. As a consequence of the uniaxial symmetry of a doublet, the frequency of this oscillation is twice the angular frequency of the magnetic field, as explained in figure 4. Because a laser beam is focused inside the cuvette, the amount of light scattered by the clusters will oscillate. This oscillating light signal is detected by a photodiode, and the amplitude of the measured signal is related to the concentration of the target molecule.

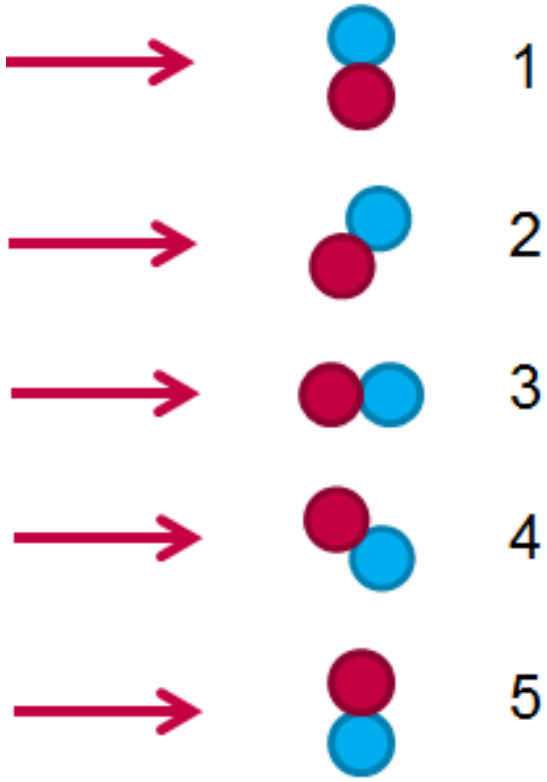

Figure 4: Scattering area of a doublet for a magnetic field frequency below the critical frequency. The arrow indicates the direction of the laser beam. In the first state, the scattering area of the doublet is maximal, while in the third state it is minimal. In the fifth state the scattering area is maximal again, although the doublet has only made a half rotation yet. As a result of this twofold symmetry of the clusters, the amplitude of the scattered light oscillates with a frequency two times as high as the angular frequency of the magnetic field.

2.5 Resulting signal and processing

An example of a signal coming from the photodiode can be seen in figure 5. This is the result of a magnetic field rotating at 6 Hz. Indeed, the frequency of the resulting signal is twice this angular frequency of the rotating magnetic field. The Fast Fourier Transform (FFT) of this signal is presented in figure 6. The Fourier transform is a mathematical application which shows what frequency components are present in a certain signal. For instance a perfect sine wave has a Fourier transform of zero everywhere, except at the frequency of the sine wave, where there is a peak. Due to the uniaxial symmetry of the doublets, the 2f peak (twice the angular frequency of the magnetic field) has a very high amplitude, and it will be taken as a measure for the amount of clusters in the assay.

If two of these measurements are performed for a range of frequencies from 1 to 25 Hz, and the amplitude of the 2f peaks in the FFT spectra is plotted as a function of this frequency, the result will be a graph like the one shown in figure 7. The MATLAB scripts which generate such graphs are shown in appendix F. The critical frequency can be seen as the point where the signal starts decreasing. This is because just above the critical frequency, the motion of the clusters changes from rotating to wiggling. Their scattering area is not oscillating with the frequency of twice the angular frequency of the magnetic field anymore, and the 2f signal drops.

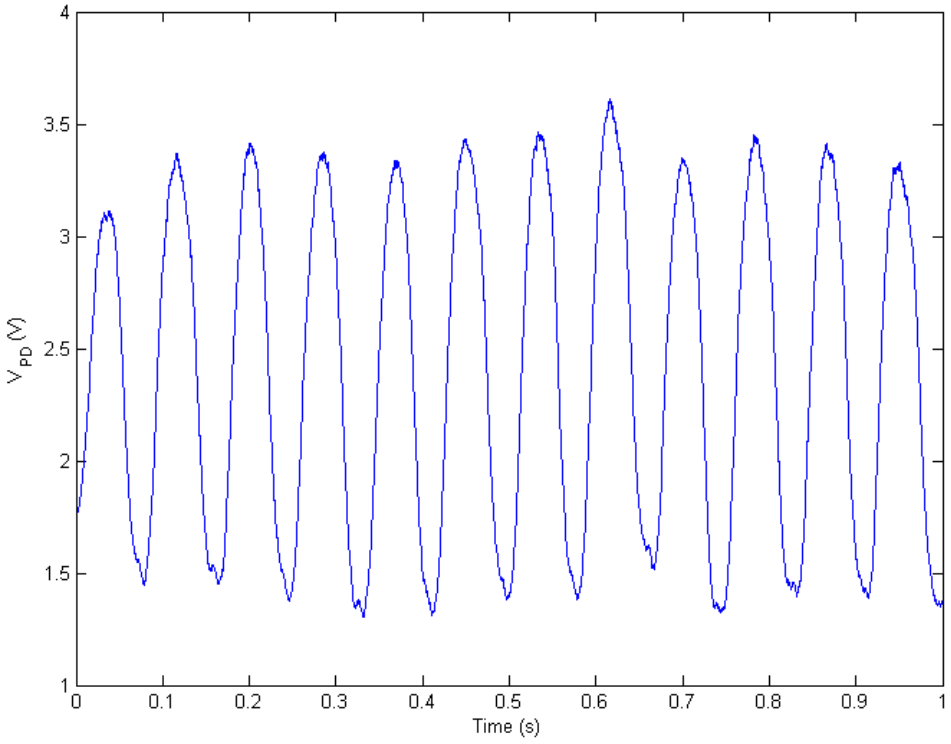

Figure 5: An example of a signal coming from the photodiode. This particular graph is the result of a measurement performed with a magnetic field rotating at 6 Hz. It can be seen that the signal coming from the diode indeed has a main frequency component of 12 Hz, due to the twofold symmetry of most of the clusters. The assay used in this measurement contained of PBS as buffer, 1% BSA, 0.5% Tween® 20 and 50 pM target. The used chaining field amplitude is 11.4 mT.

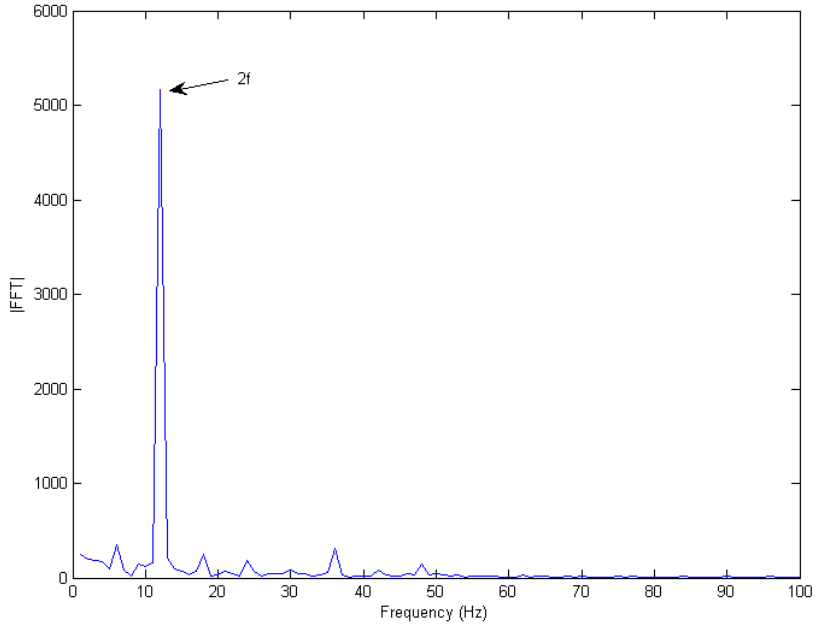

Figure 6: The FFT of the signal shown in figure 5. The assay used in this measurement contained of PBS as buffer, 1% BSA, 0.5% Tween® 20 and 50 pM target. The used chaining field amplitude is 11.4 mT. It can be seen that the 2f peak in this spectrum has a very high amplitude. This is, again, due to the uniaxial symmetry of doublets, which account for the frequency of the photodiode output to be twice as high as the angular frequency of the magnetic field.

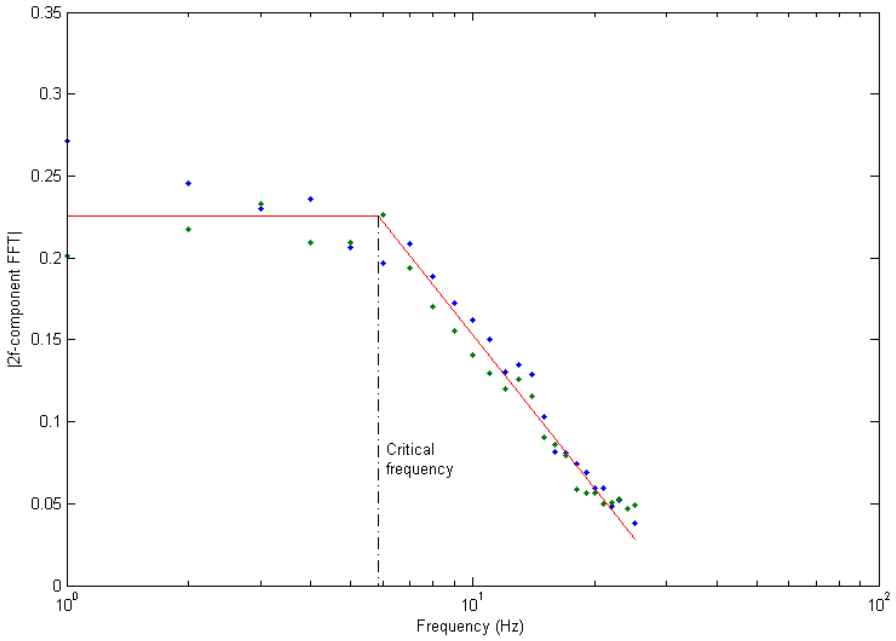

Figure 7: The amplitude of the 2f peak in the FFT spectrum plotted as a function of the angular frequency of the rotating magnetic field. The critical frequency can clearly be seen as the point where the signal starts decreasing. This is because the clusters are wiggling instead of rotating. Their scattering area is not oscillating with the frequency of two times the angular frequency of the magnetic field anymore, so the 2f signal drops.

3. Experimental setup

3.1 General setup

The most important part of the used setup is shown in figure 8. In the middle is the glass cuvette containing the assay. Around this cuvette are the four coils which generate the magnetic field. The bright red line is the laser beam, which is focused on a small volume inside the cuvette, and the pale red beam is the scattered light which leads to the photodiode pictured on the right. A Thorlabs LDC 205 C laser diode controller is used to control the current to the used 120 mW, 660 nm laser diode: an Opnext HL6545MG. LabVIEW software is used to control the magnetic field coils via a voltage to current amplifier. The signal sent to each coil is a sinusoidal signal, which has a phase shift of ninety degrees with respect to the next coil. This creates a magnetic field rotating in the xz-plane as shown in figure 8. Three photodiodes are used in the setup: one to measure the transmitted laser light, one that is fixed at a 30 degree angle with respect to the transmitted laser beam, and one that can be adjusted to have an angle between 60 and 130 degrees with respect to the laser beam.

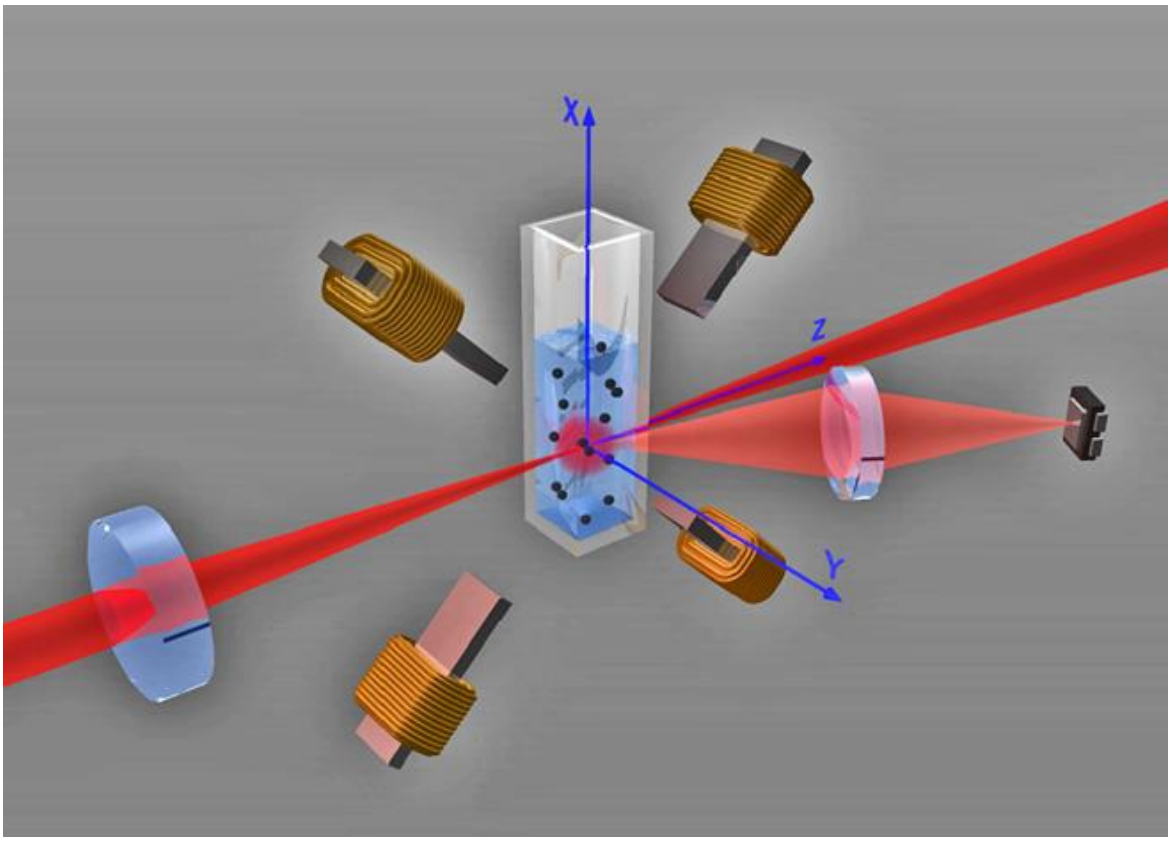

Figure 8: The most important part of the experimental setup. In the middle is the glass cuvette containing the assay. Around this cuvette are the four coils which generate the magnetic field. The bright red line is the laser beam, which is focused on a small volume inside the cuvette, and the pale red beam is the scattered light which leads to the photodiode pictured on the right.

3.2 Experiments: general

In all experiments, the used buffer is phosphate buffered saline (PBS), the used target is biotinylated bovine serum albumin (bBSA), and the used superparamagnetic beads are Invitrogen Dynabeads MyOne Streptavidin C1 with a diameter of one micrometer (stock concentration 10 mg/ml). The streptavidin on this beads has a very high affinity for the biotin on the target. The magnetic properties of the beads make it possible to remove the fluid the beads are immersed in, wash the beads, and immerse them in a buffer fluid of known composition.

In the experiments, the chaining step takes two minutes, containing twenty pulses of the magnetic field. The magnetic field in this step has a frequency of 1 Hz, an on-time of two seconds, and an off-time of four seconds. The amplitude of this field is optimized. Next, there is a minute in which no field is applied, which gives the particles the chance to redistribute randomly again, as the chaining step has brought them close together. Thereafter the actual measurement begins. The rotating field in this measurements has an on-time of one second and an off-time of five seconds. The amplitude of this field is 5 mT. The first pulse has a frequency of 1 Hz, and with each pulse the frequency increases with one Hertz. After the pulse of 25 Hz, this frequency sweep starts over again for a second series of 25 pulses.

3.3 Experiments: optimization of the assay

In the process of optimization of the assay, the purpose is to keep the amount of formed non-specific clusters as low as possible, without completely suppressing the formation of the wanted, specific bonds. This means that the values of the resulting graphs as shown in figure 7 should be as low as possible in the case when there is no target present in the assay. The rate between the resulting signal with target in the assay and the signal without target in the assay should be as high as possible.

The first attempted method to optimize the assay is adding different concentrations of bovine serum albumin (BSA) to the buffer. It is hoped that this BSA will non-specifically cover the surface of the beads on the places where non-specific binding is most likely, blocking these places for non-specific bonds between the particles.

The second method is changing the amplitude of the pulsating magnetic field that is used in the magnetic chaining step. A lower amplitude means that the beads are pulled together less strongly, which may result in a lower amount of non-specific bonds, but maybe also in less specific bonds. The rate between these two binding types has to be optimized.

Other possibilities are adding biotinylated polyethylene glycol (PEG) or polysorbate 20 (Tween® 20) to the beads. Biotinylated PEG will bind to the streptavidin on the surface of the beads, blocking a part of the binding places for target molecules. Because the PEG also forms a brush around the particles, the formation of non-specific bonds is reduced too. Tween® 20 sticks to the surface of the beads non-specifically, blocking other non-specific bonds.

The last method that is attempted to optimize the assay is lowering the salt concentration in the buffer. This is done by diluting the used PBS with demineralized water. Diluting the PBS means a lower ionic strength, and thus a higher Debye length [7]. Because the particles are negatively charged at neutral pH they have an electric field, which keeps them separated. This electric field of the used particles decreases exponentially with the Debye length, so a lower salt concentration means more repulsion between the particles. However, lowering the salt concentration can also make it harder for the superparamagnetic particles to capture the bBSA target, which would reduce specific binding as well.

3.4 Experiments: dose response, microscopy and angular dependence

Using the optimized parameters found in these experiments, a dose response curve is measured. This curve gives the relation between the concentration of target and the 2f Fourier component at a specific measuring frequency.

Next, the Leica DM6000 M microscope and the Neo sCMOS camera are used to make pictures of assays containing different concentrations of target molecules. Per concentration, six pictures like figure 9 are made and the beads are counted and labeled: singlet, doublet or bigger cluster. This is done right after the magnetic chaining step, so the rates of single beads, doublets and bigger clusters in an assay that is normally used for a measurement can be calculated after counting the particles by hand.

The last performed experiment is measuring the angular dependence of the light scattering. The same measurement is performed several times, but with the adjustable photodiode at a different angle. The optimized assay is used again.

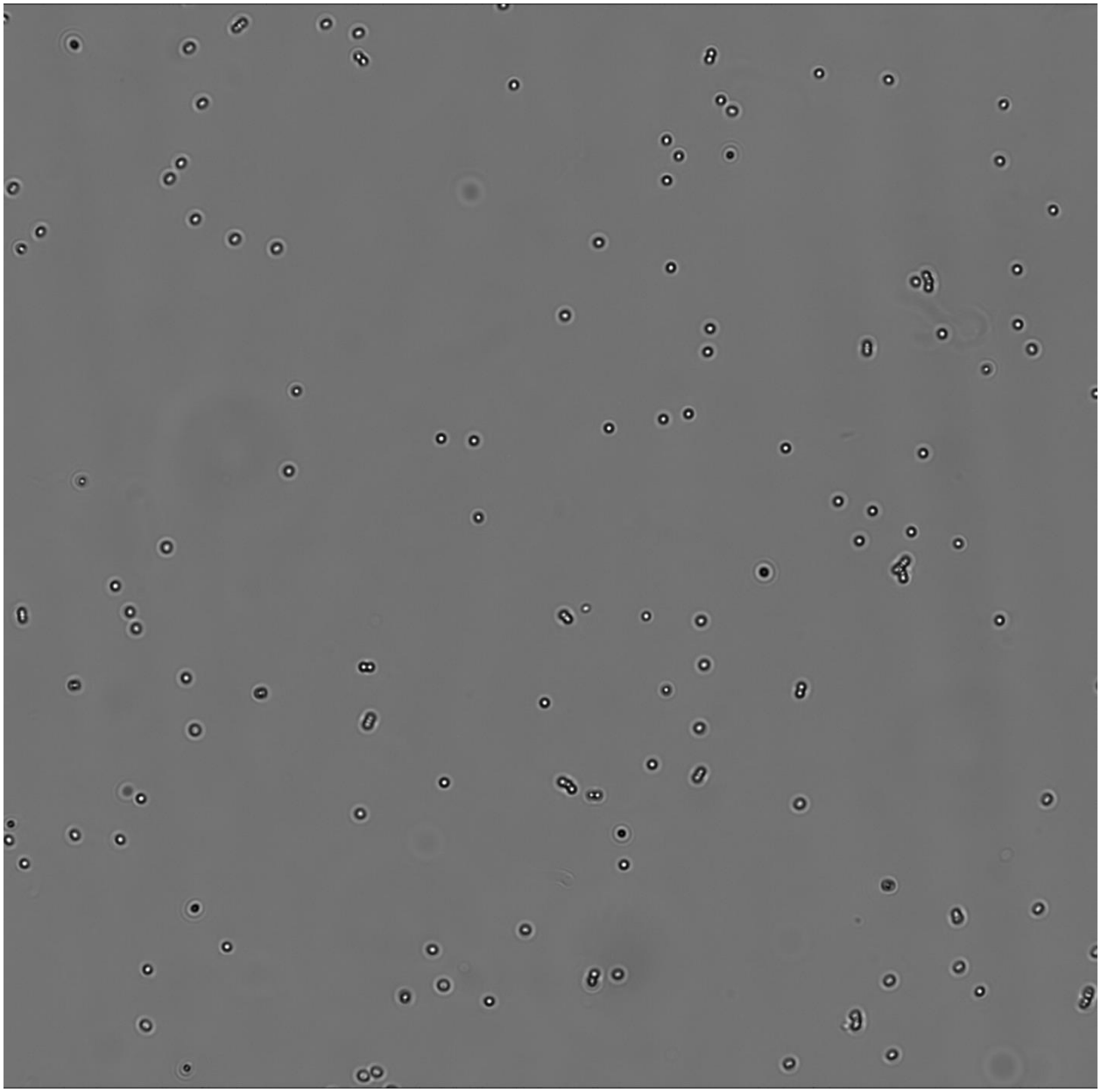

Figure 9: A picture of the optimized assay that went through the magnetic chaining step. This picture is made using the Leica DM6000 M microscope and the Neo sCMOS camera. Either single particles, doublets and larger particles can clearly be distinguished.

4. Results and discussion

4.1 Optimization: BSA concentration

In the first experiment, the BSA concentration in the assay is optimized. Measurements are performed on assays containing 0.208%, 0.55%, 1%, 1.9% and 4.6% BSA. These measurements are done without target, so that the resulting signal is entirely the result of non-specific clusters. The used superparamagnetic beads are washed two times using buffer containing the specific amount of BSA, and diluted fifty times. Two examples of resulting graphs are shown in appendix A, and the final graph is shown in figure 10. It follows, that in the measurements using the first three concentrations, the signal lowers with increasing BSA concentration. A BSA concentration higher than 1% has no significant effect, so in the following measurement, this concentration is used.

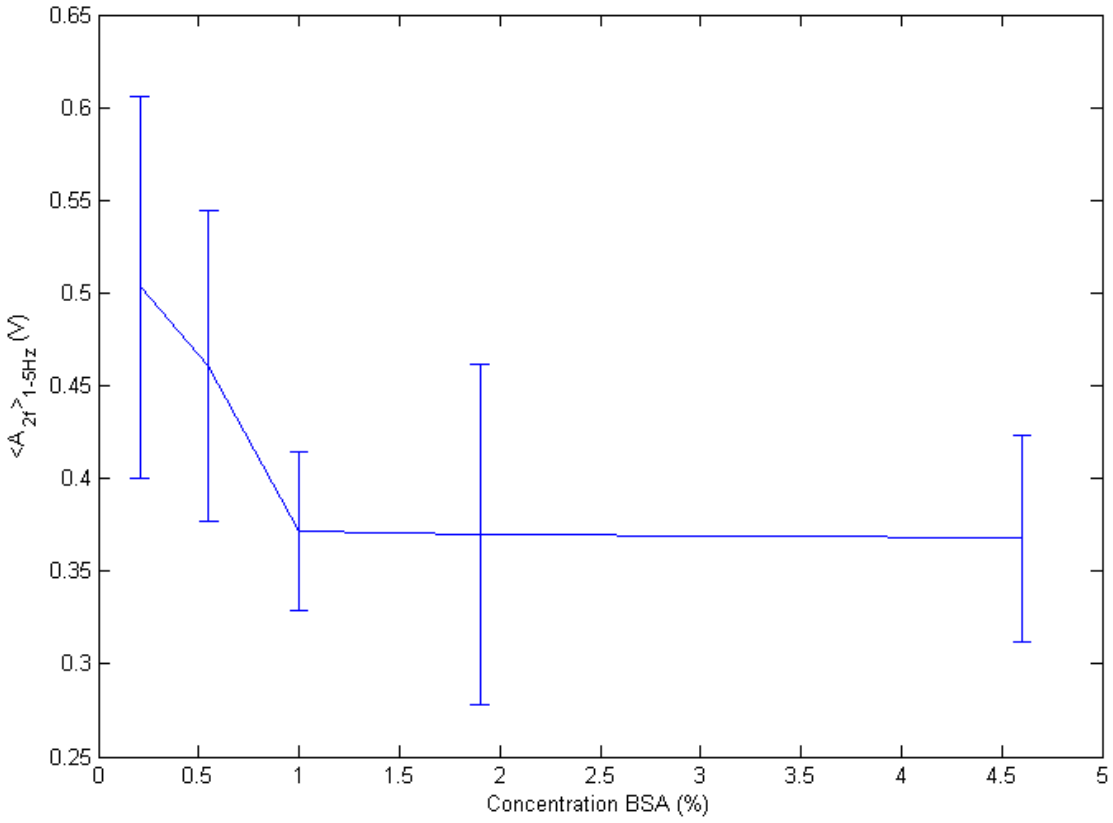

Figure 10: The amplitude of the 2f-component in the Fourier transforms of the photodiode signal as a function of the BSA concentration. A BSA concentration higher than 1% does not significantly lower non-specific binding.

4.2 Optimization: chaining field amplitude

The following experiment involved variation of the amplitude of the magnetic field in the chaining step. This amplitude is lowered from 25 mT to 21.6, 18.2, 14.8, 11.4 and 8 mT. Again, there is no target present in the assay, and the beads are washed two times using buffer containing 1% BSA and diluted fifty times. Two examples of resulting graphs can be seen in appendix B. Lowering the field amplitude does not have a strong effect at first. However, going beneath 18.2 mT, the signal starts to decrease. See figure 11, and mind the inverted x-axis. Obviously, less clusters are formed because the superparamagnetic beads are not pulled together as strongly as before. This also has less specific clusters as a consequence. To see whether there are still some of these clusters formed, a specific measurement is performed using a field of 8 mT. In figure 12, the dose response curve is shown for a measuring frequency of 3 Hz. Indeed, the signal keeps increasing as a function of the target concentration, which indicates specific clusters.

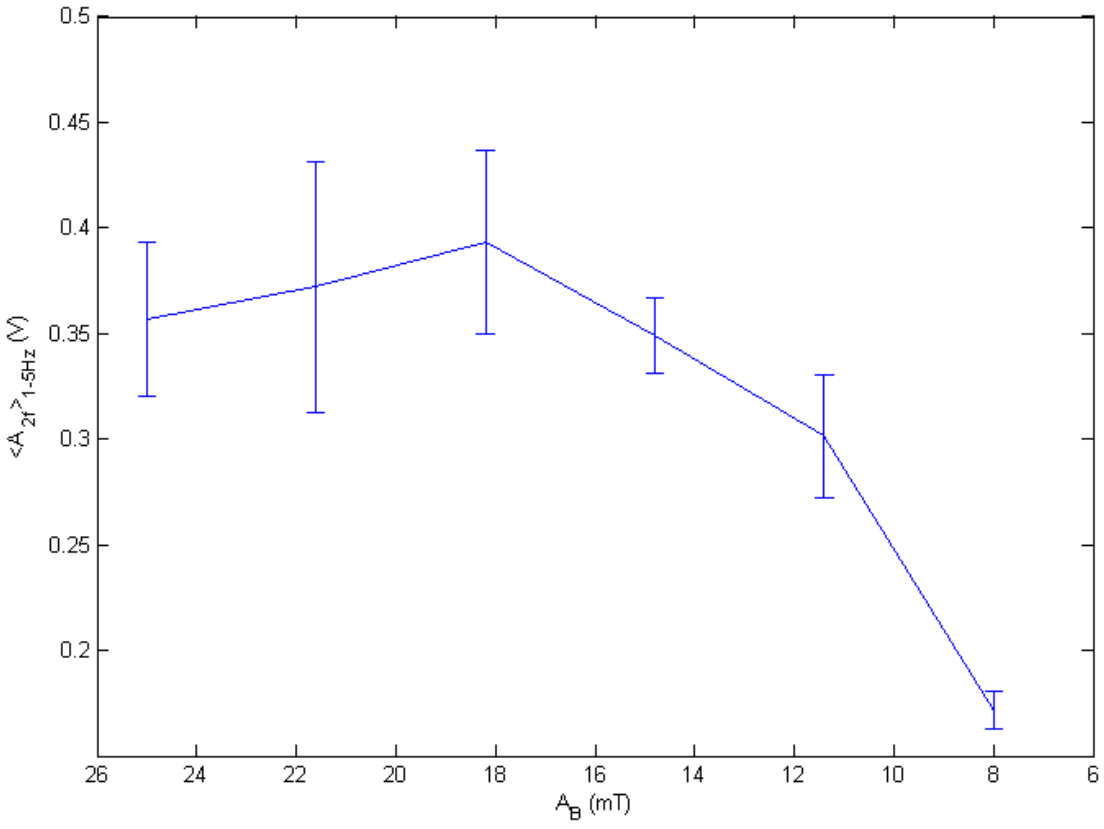

Figure 11: The amplitude of the 2f-component in the Fourier transforms of the photodiode signal as a function of the chaining field amplitude.

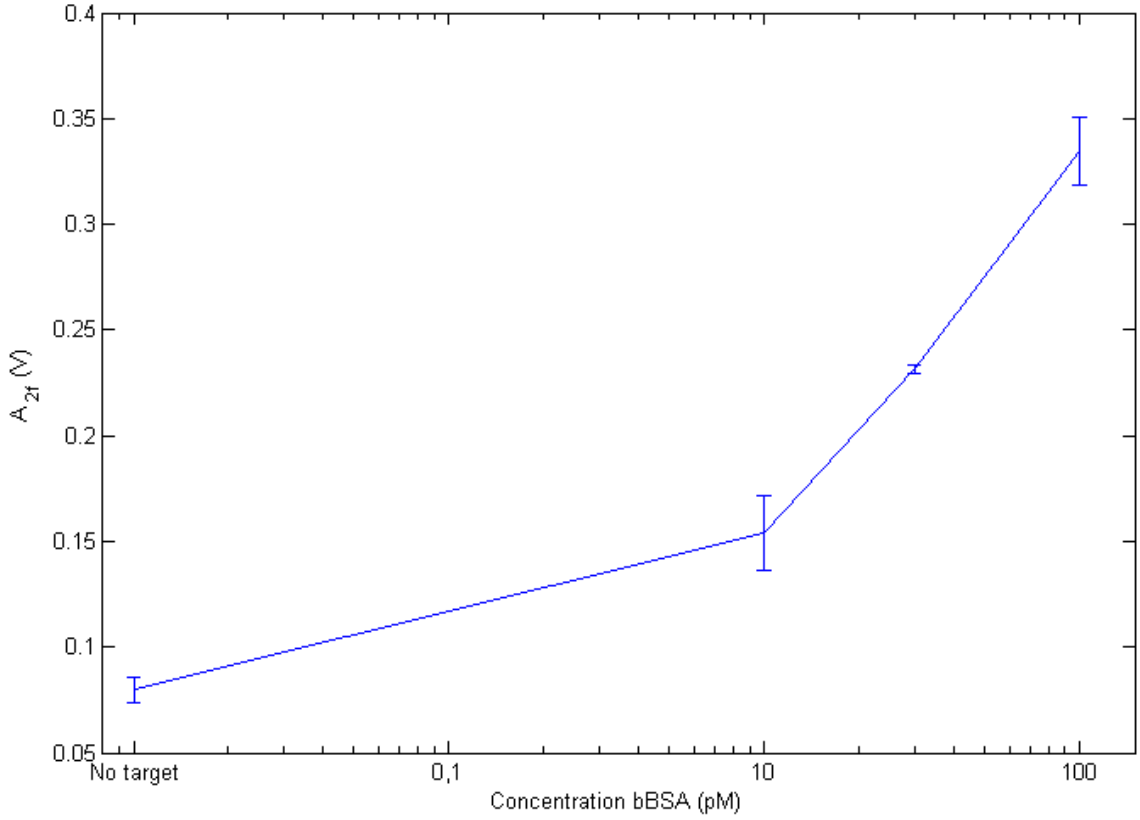

Figure 12: The dose response curve measured for a BSA concentration of 1%, an amplitude of the chaining field of 8 mT, a measuring frequency of 3Hz, and 50 times diluted beads.

The amplitude of the 2f peak of the FFT of the photodiode signal in figure 12 is very low, and needs to be increased so that noise has less impact. In order to achieve this, the magnetic field used for the chaining step needs to be increased, without increasing the amount of non-specific clusters.

4.3 Optimization: PEG concentration

The first method that is tried to achieve this, is adding PEG to the beads. In appendix C, a few of the resulting graphs for the non-specific measurements involving PEG are shown. Concentrations of 0, 10, 30, 100 and 300 µM are used, and the incubation time is 10 minutes. The signals are lower than before, which is because in this experiment, the beads are diluted 100 times instead of 50 times. It can be seen that adding a small amount of PEG indeed lowers the amount of non-specific bonds, because those signals are smaller than the signal from the same measurement with 0 µM PEG. Too much PEG, for instance 300 µM, does not have the desired effect, as the characteristic form of the graph, in which the critical frequency can be seen, is lost. This is probably because noise begins to play a significant role.

Specific measurements are performed using a small magnetic field and different concentrations of PEG, but the difference between the case with and without target cannot be observed. So indeed, the magnetic field amplitude has to be increased. When this is done, however, still no significant increase is seen when target is added. In an attempt to resolve this problem, two times as much beads are added to the assay. The dose response curves for PEG concentrations of 10 and 100 µM are shown in figures 13 and 14.

As can be seen from these graphs, 10 µM PEG does not sufficiently block the non-specific interactions, so that it is impossible to see the difference between an assay with target and an assay without target. When 100 µM PEG is used, the ratio between the signal with a certain amount of target and the blank signal is lower than this ratio as seen in figure 12, without PEG. Some more similar measurement are performed, but without the desired results. The last performed experiment involving PEG, is checking at which PEG concentration the resulting photodiode signal becomes independent of the amplitude of the magnetic field used in the chaining step. It turns out that this is never the case, at none of the used concentrations. From this point on, no more PEG is used.

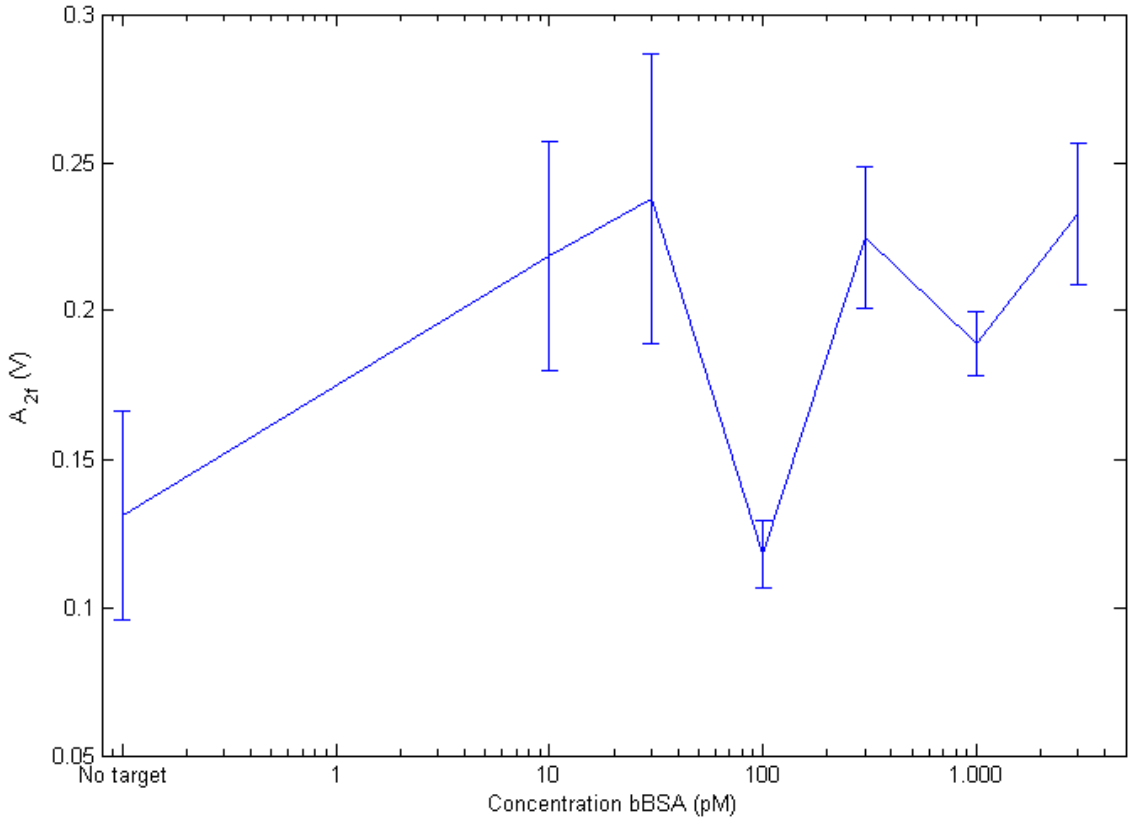

Figure 13: The dose response curve measured for a BSA concentration of 1%, an amplitude of the chaining field of 25 mT, a measuring frequency of 3Hz, a PEG concentration of 10 µM and 50 times diluted beads.

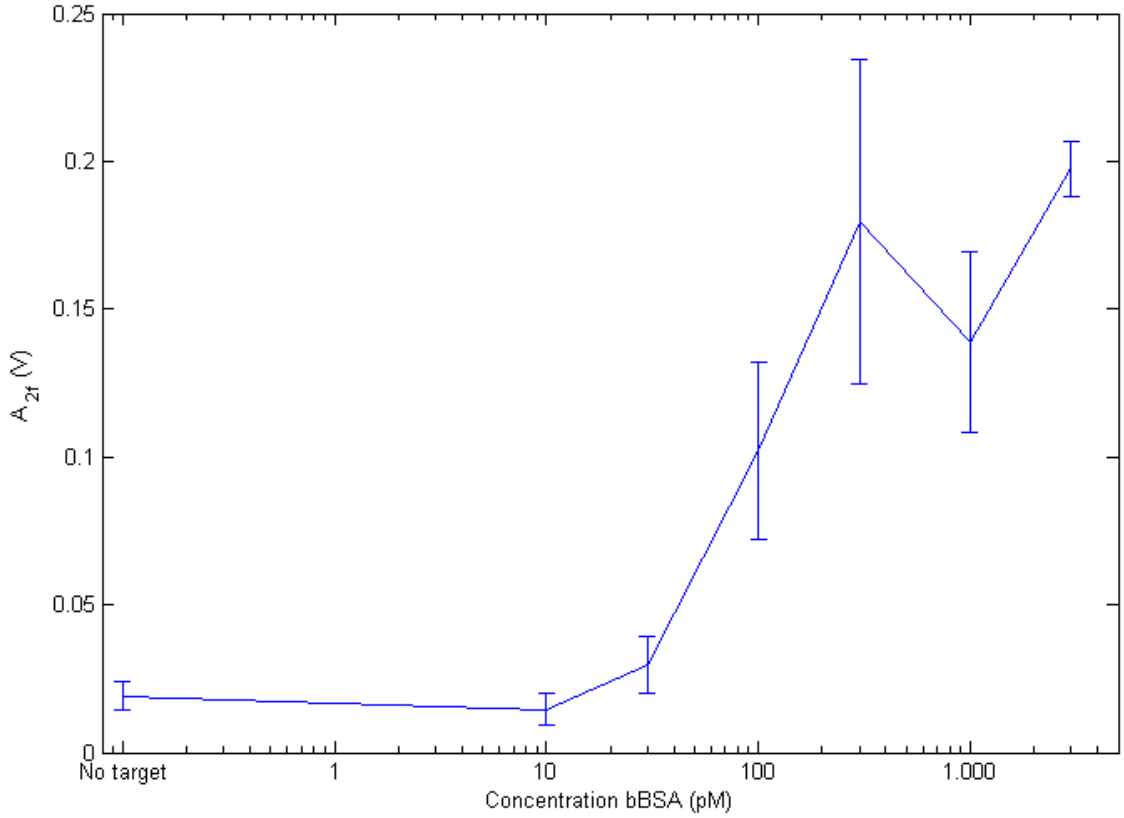

Figure 14: The dose response curve measured for a BSA concentration of 1%, an amplitude of the chaining field of 25 mT, a measuring frequency of 3Hz, a PEG concentration of 100 µM and 50 times diluted beads.

4.4 Optimization: Tween® 20 concentration

The next attempted manner to improve the ratio of the signal with target and the signal without target, is adding Tween® 20 to the assay. From the examples of resulting graphs in appendix D can be seen that Tween® indeed blocks non-specific bindings, as the signal from a measurement without target lowers with increasing Tween® concentration. Also, Tween® has a positive effect on the desired ratio. The best ratio is achieved using a concentration of 0.5% Tween®. This is shown in figure 15. The next step is to determine what is the best amplitude for the magnetic field in the magnetic chaining step, using Tween®. Some of the graphs are shown in appendix E. The best amplitude turns out to be 11.4 mT, as the ratio between the signal of the specific measurement and the blank measurement is the highest in this case.

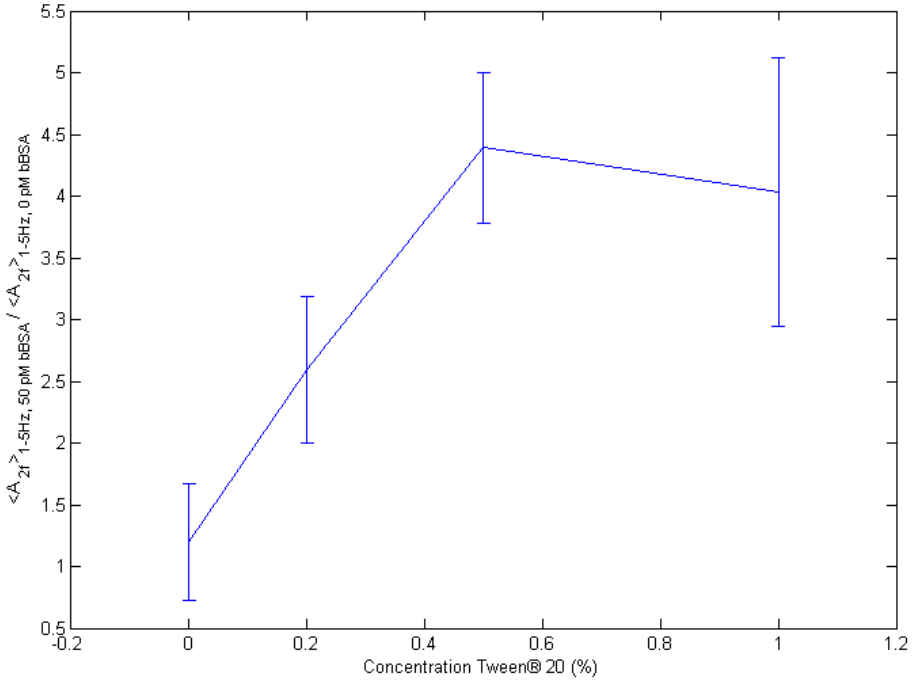

Figure 15: The ratio of the amplitude of the 2f-component in the Fourier transforms of the photodiode signal for a measurement done using 50 pM target, and a measurement done using no target, as a function of the Tween® 20 concentration.

4.5 Optimization: salt concentration

One last parameter that is varied, is the salt concentration of the assay. This is done by diluting the PBS used as buffer. This does not help, as already at ten times dilution, the ratio between the specific signal and the blank signal drops to one. All specific interactions are apparently blocked. Hence, normal PBS remains to be used as the buffer fluid.

A list of optimized parameters is shown in table 1.

Parameter	Value
BSA concentration	1%
Chaining field amplitude	11.4 mT
PEG concentration	0 M
Tween® 20 concentration	0.5%

Table 1: the values of the optimized parameters.

4.6 Dose response

After the optimization, measurements are performed in order to make a dose response curve. The target concentration is varied in a range from 0 to 2 nM. With each target concentration, three measurements are performed. The blank measurement is performed five times. The resulting graph is pictured below, in figure 16. This graph involves measurement frequencies from 1 to 5 Hz. From the graph, it follows that the minimum concentration of target that can reliably be detected is 5 pM. The highest concentration of target than can reliably be detected is 50 pM. At this point, the saturation level is reached.

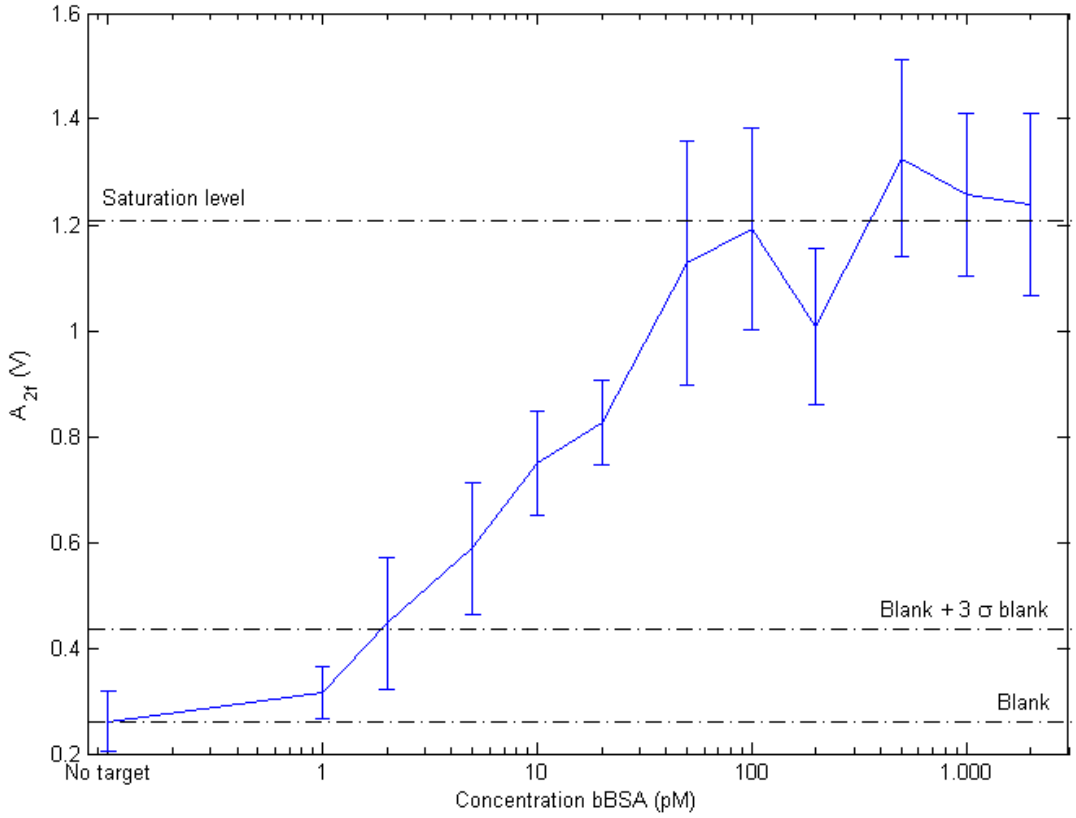

Figure 16: The resulting dose response curve, measured with the optimized assay. This graph involves measurement frequencies from 1 to 5 Hz. The minimum concentration of target that can reliably be detected is 5 pM. The highest concentration of target than can reliably be detected is 50 pM. At this point, the saturation level is reached.

4.7 Microscopy

As explained in the experimental setup, the experiments conducted next involved microscopy. Four target concentrations are examined: 0, 1, 10 and 100 pM. Per concentration, six pictures like figure 9 are made and the clusters are counted and categorized: singlet, doublet or bigger cluster. The particles are categorized manually. A particle, or a cluster of particles, is disregarded when it is out of focus or when it is unclear what category it actually belongs to. In figure 17, typical appearances are shown. The relative amount of single particles, doublets and clusters is shown in the bar chart of figure 18. The amount of doublets and larger clusters indeed grows as a function of the target concentration, which matches the preceding expectations and experimental results.

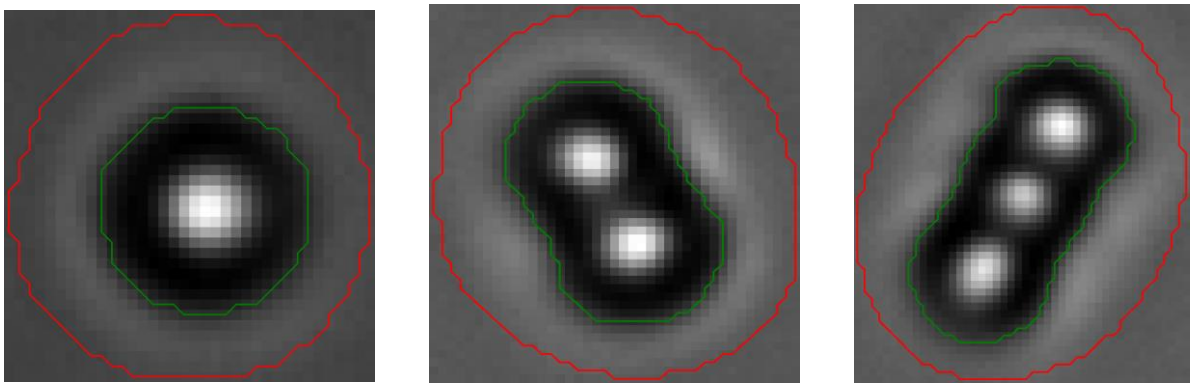

Figure 17: A typical single particle, doublet and bigger cluster (a triplet in this case), as seen through the Leica DM6000 M microscope.

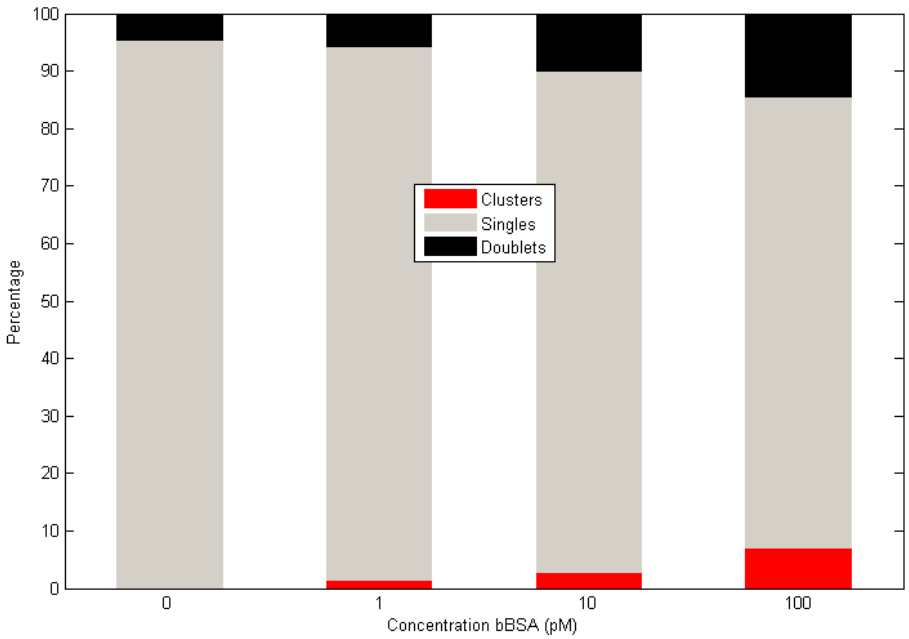

Figure 18: Bar chart of the relative amounts of single particles, doublets and clusters as a function of the concentration of the target molecules.

4.8 Angular dependence

For the last part of this project, the angular dependence of the light scattering of the assay is measured. The measurements are performed during 100 magnetic field pulses of 5 Hz, and the angle of one of the photodiodes is varied in a range from 60 to 130 degrees. The first time, all experiments are conducted using 50 pM of bBSA, and 100 times diluted beads. Some of the resulting graphs are shown in figure 19. It can be seen that a prominent result of this experiment is the fact that each photodiode angle has its own specific form of the resulting graph. To check whether this form depends on the target concentration somehow, the same experiments are conducted twice more: one with ten times less target, and one with three times less target and also three times less beads, so the ratio between target and beads stays the same. It turns out that these last two experiments have similar results, which differ from the ones obtained in the first experiment, at the point where the graphs are minimal. This difference has to be caused by the formation of clusters of beads just sticking together non-specifically.

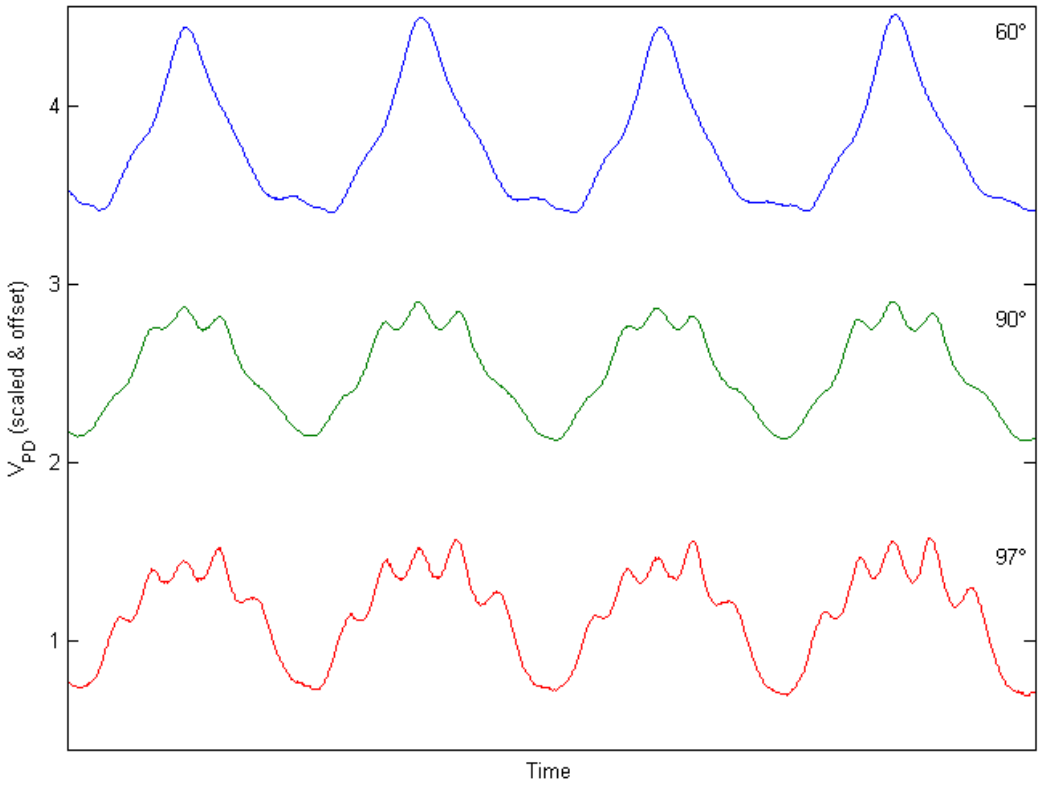

Figure 19: The photodiode signal as a function of time, as measured at different angles. The blue graph is measured at 60 degrees, the green one at 90 degrees, and the red one at 97 degrees.

In the following figures, 20 and 21, the amplitude of the various frequency components in the Fourier transforms of the photodiode signals are shown as a function of the photodiode angle. In figure 20, the values are unscaled, and in figure 21, all values are scaled with respect to the amplitude of the 2f-component. In figure 20, it can be seen that the amount of scattered light decreases as a function of the detector angle. When the angle is increased even further, the signal increases again. This is due to laser light which is scattered in a forward direction, but reflected by the glass cuvette in a backward direction. From figure 21, it follows that, at big angles around 100 degrees, the higher frequency components (10f up to 16f) play an important role, while the role of lower frequency components (4f, 6f, 8f) remains more or less equal. This matches with the fact that the photodiode signals for these angles show more peaks than the signals for small angles.

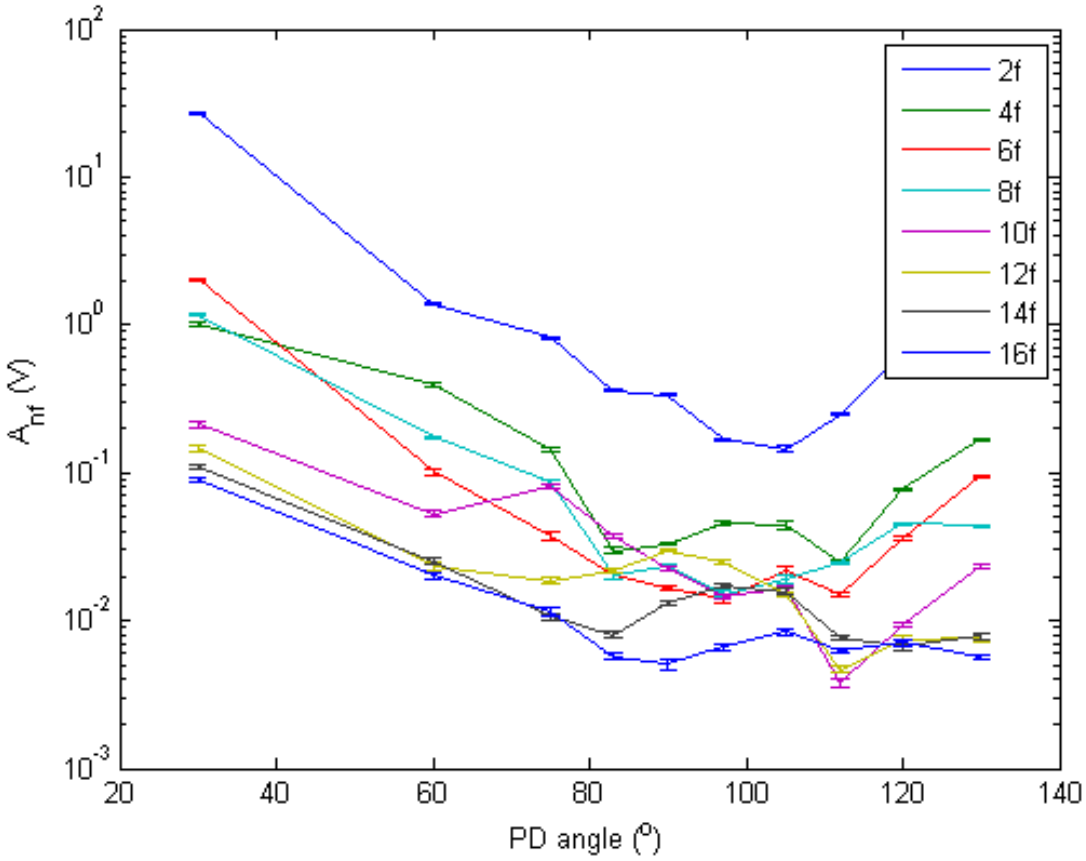

Figure 20: The amplitude of the various frequency components in the Fourier transforms of the photodiode signal, as a function of the photodiode angle. In this graph, all values are unscaled.

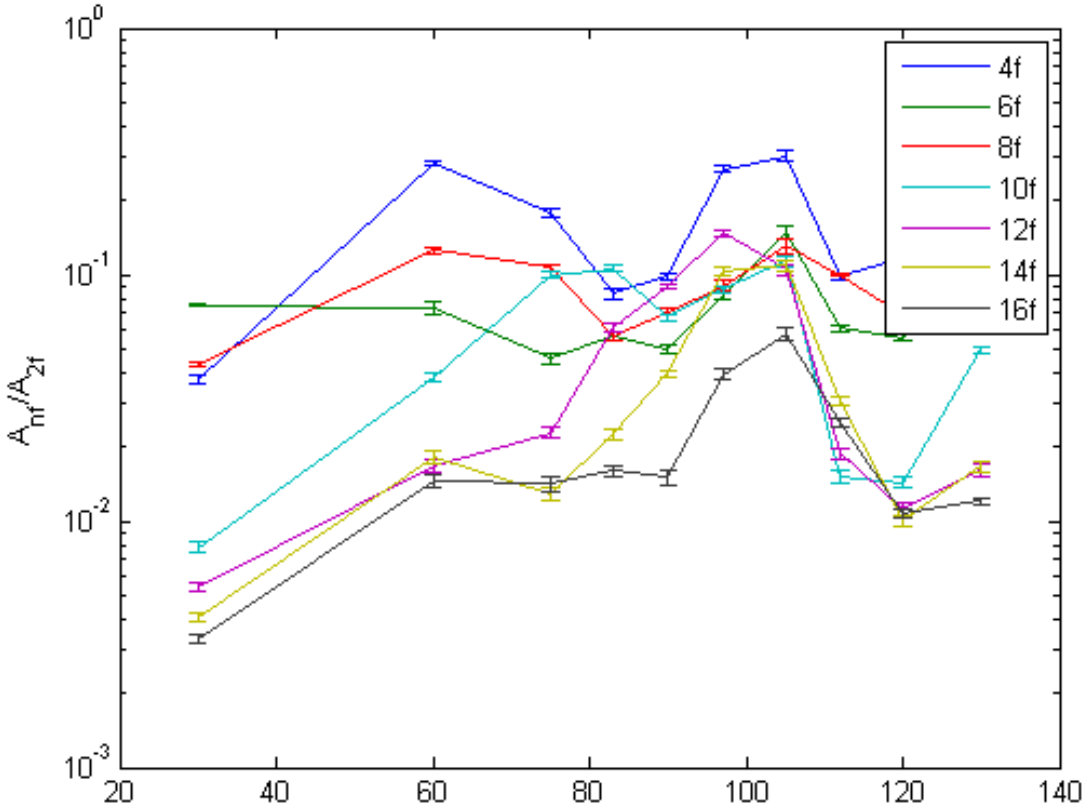

Figure 21: The amplitude of the various frequency components in the Fourier transforms of the photodiode signal, as a function of the photodiode angle. In this graph, all values are scaled with respect to the 2f-component.

5. Conclusion

In this project, an assay is optimized so that it works best for detecting a specific target molecule. The final assay consists of PBS as a buffer fluid, 1% BSA, 0.5% Tween® 20 and 0.1 mg/ml superparamagnetic beads. The amplitude of the magnetic field used for the magnetic chaining is 11.4 mT.

Using this assay and these settings, a dose response curve is made, and it follows that it is possible to accurately detect target concentrations between 5 and 50 pM.

Also, the assay is observed using a microscope, after it went through the chaining step. It is found that the amount of doublets and larger clusters indeed grows as a function of the target concentration, which matches the preceding expectations and experimental results.

The last part of this project involved measuring the angular dependence of the light scattering of the clusters. It follows that for every scattering angle, the photodiode signal has its very own shape.

When the angle of the movable photodiode is increased from 60 to 130 degrees, a change can be seen in the number of small peaks per main peak of the signal. At the lowest angles (30 and 60 degrees), only one peak is present. At 90 degrees there are clearly three visible peaks, and at 97 degrees even five peaks are observed. These peak disappear if the angle is increased even more.

At angles around 90 degrees, the total amount of detected light is low, but the higher frequency components of the Fourier transform of the photodiode signal play a more significant role than at small angles. This gives rise to the increased amount of peaks that are present in the photodiode signal. When the angle is increased even more, the total amount of scattered light increases again. This is the result of light scattered in a forward direction, but reflected by the glass cuvette in a backward direction.

Bibliography

[1] S. Wild, G. Roglic, A. Green, R. Sicree and H. King, “Global prevalence of diabetes: Estimates for the year 2000 and projections for 2030”, *Diabetes Care*, vol. 27, pp. 1047-1053, May 2004.

[2] J.M. van Kemenade, “Study of length-dependent magnetic and optical properties of rotating particle chains”, April 2012.

[3] http://www.libertymedical.com/uploadedimages/products/diabetes/LIFSP021911NC/lifescan-onetouch-ultramini-blood-glucose-monitoring-system-3.jpg.

[4] F.L. Calderon, T. Stora, O.M. Monval, P. Poulin and J. Bibette, “Direct measurement of colloidal forces”, *The American Physical Society*, vol. 72, pp. 2959-2962, May 1994.

[5] J. Baudry, C. Rouzeau, C. Goubault, C. Robic, L. Cohen-Tannoudji, A. Koenig, E. Bertrand and J. Bibette, “Acceleration of the recognition rate between grafted ligands and receptors with magnetic forces”, *Proceedings of the National Academy of Sciences of the United States of America*, vol. 103, no. 44, pp. 16076-16078, 2006.

[6] A. Ranzoni, “Rotational actuation of magnetic nanoparticle clusters for solution-based biosensing”, 2012.

[7] P. Debye and E. Hückel, “The theory of electrolytes ”, *Physikalische Zeitschrift*, vol. 24, pp. 185-206, 1923.

Appendix A: results of the variation of the BSA concentration

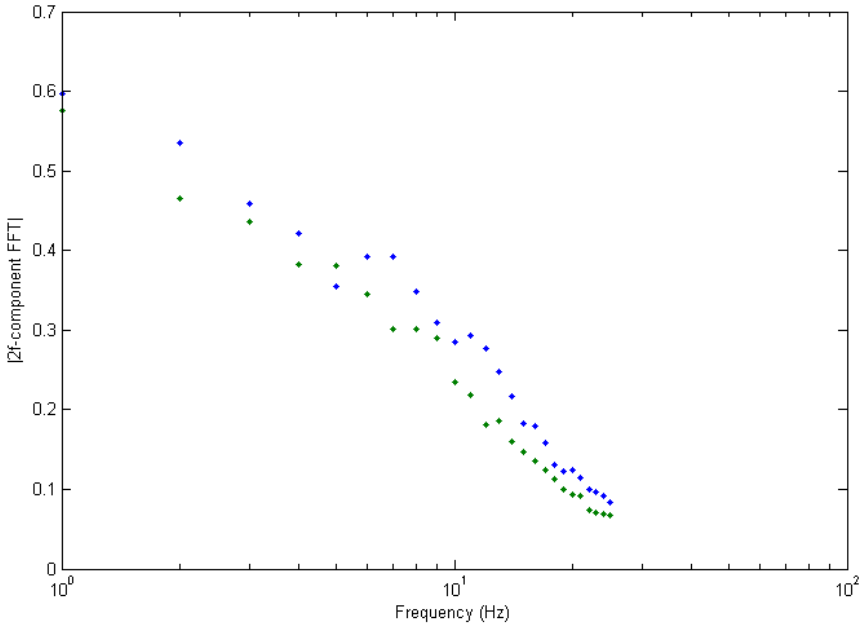

Figure A.1: The resulting graph of a measurement done using PBS as buffer, 50 times diluted beads, no target, a chaining field amplitude of 25 mT and a BSA concentration of 0.55%.

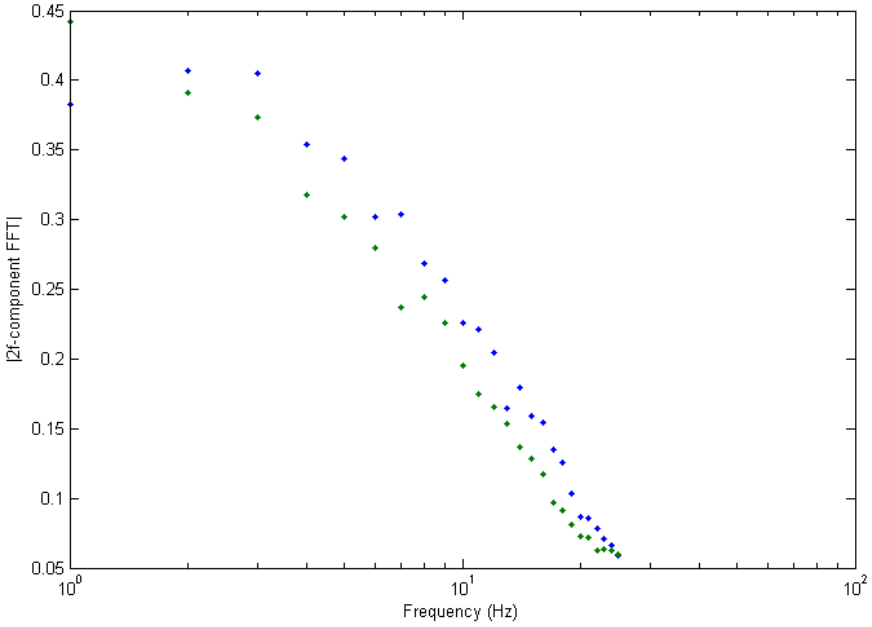

Figure A.2: The resulting graph of a measurement done using PBS as buffer, 50 times diluted beads, no target, a chaining field amplitude of 25 mT and a BSA concentration of 1%.

Appendix B: results of the variation of the chaining field amplitude

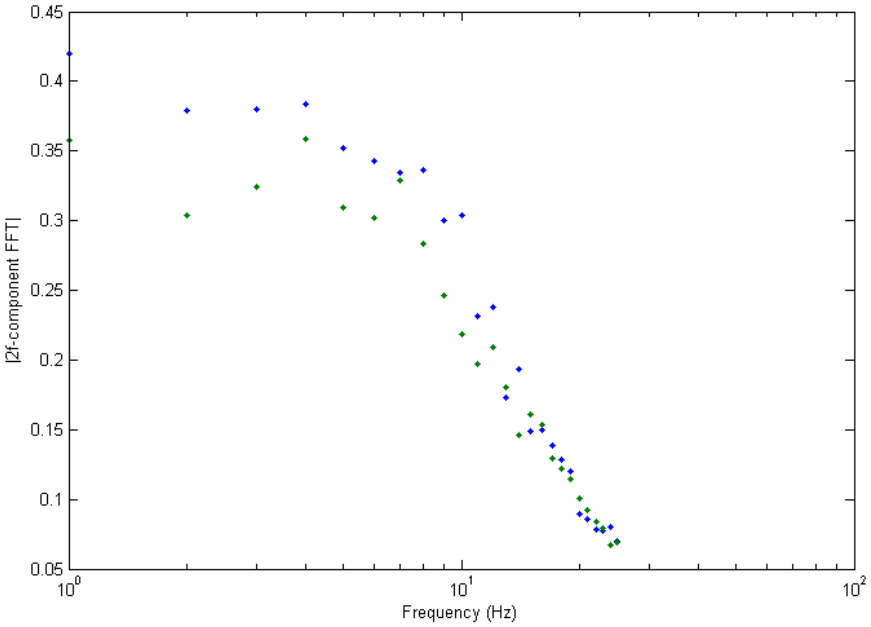

Figure B.1: The resulting graph of a measurement done using PBS as buffer, 50 times diluted beads, no target, a chaining field amplitude of 25 mT and a BSA concentration of 1%.

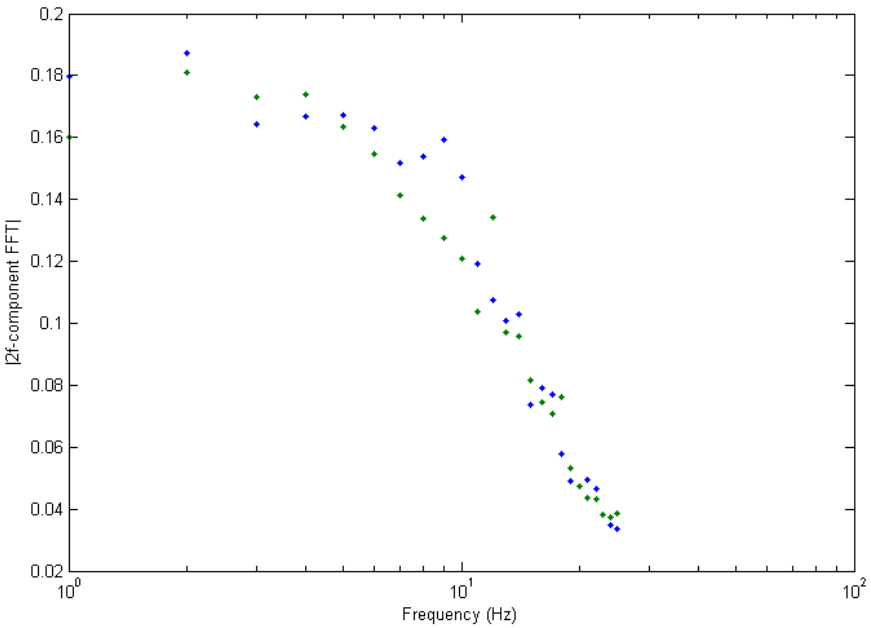

Figure B.2: The resulting graph of a measurement done using PBS as buffer, 50 times diluted beads, no target, a chaining field amplitude of 8 mT and a BSA concentration of 1%.

Appendix C: results of the variation of the PEG concentration

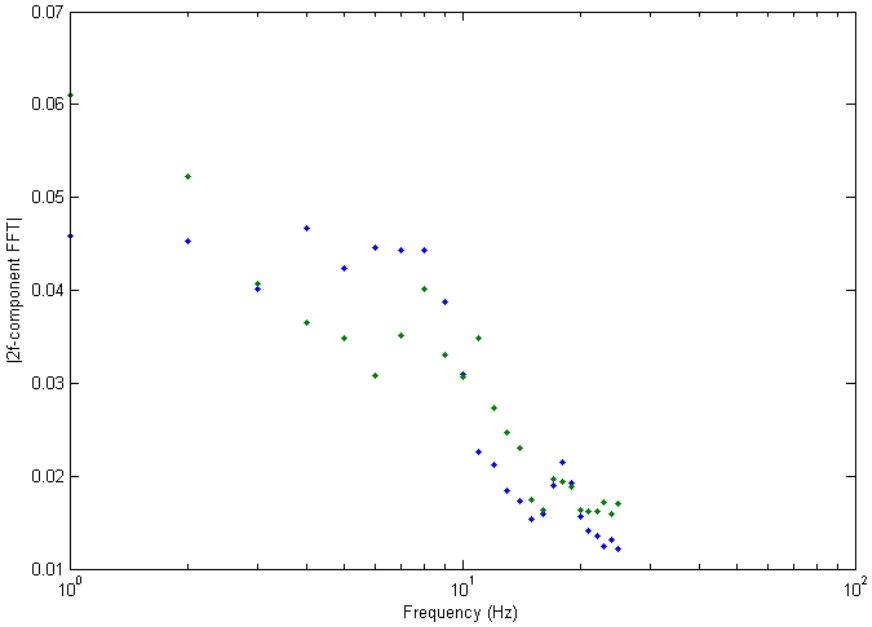

Figure C.1: The resulting graph of a measurement done using PBS as buffer, 100 times diluted beads, no target, a chaining field amplitude of 8 mT , a BSA concentration of 1% and a PEG concentration of 0 µM.

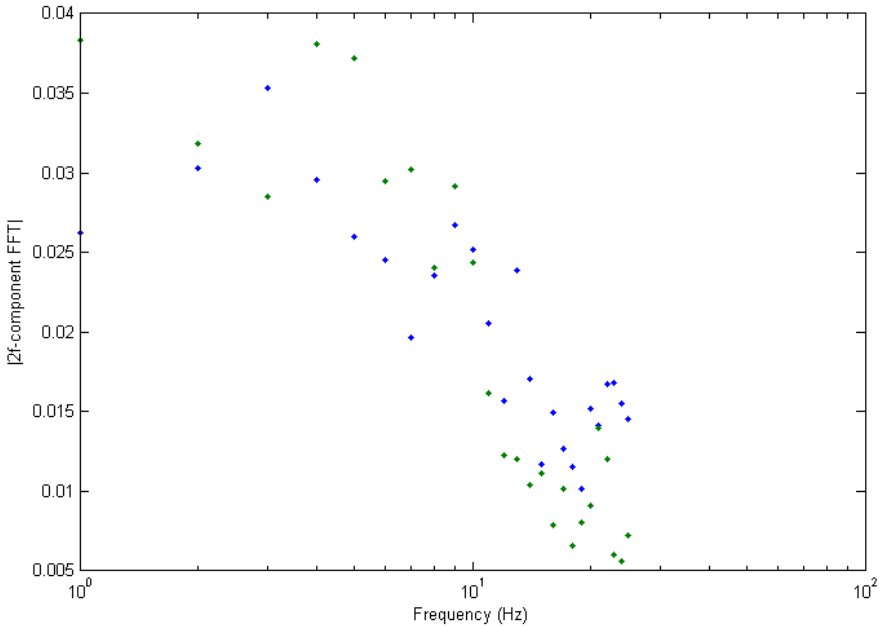

Figure C.2: The resulting graph of a measurement done using PBS as buffer, 100 times diluted beads, no target, a chaining field amplitude of 8 mT, a BSA concentration of 1% and a PEG concentration of 30 µM.

Appendix D: results of the variation of the Tween® 20 concentration

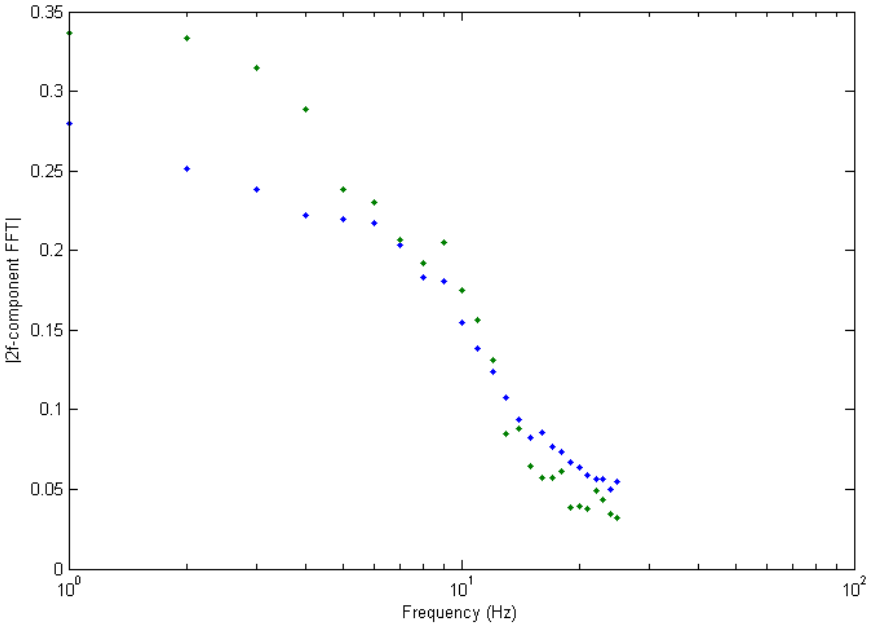

Figure D.1: The resulting graph of a measurement done using PBS as buffer, 100 times diluted beads, 0 pM target, a chaining field amplitude of 25 mT, a BSA concentration of 1% and 0% Tween® 20.

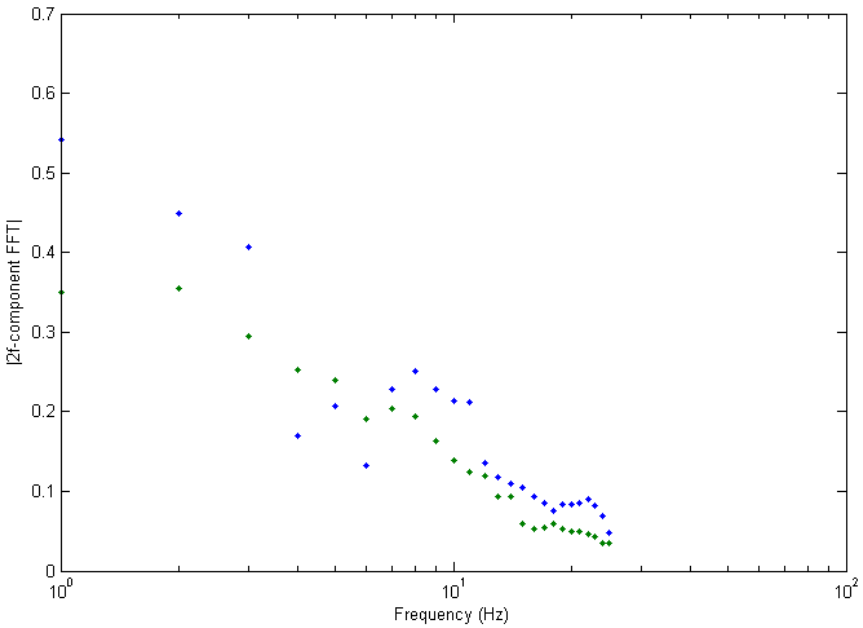

Figure D.2: The resulting graph of a measurement done using PBS as buffer, 100 times diluted beads, 50 pM target, a chaining field amplitude of 25 mT, a BSA concentration of 1% and 0% Tween® 20.

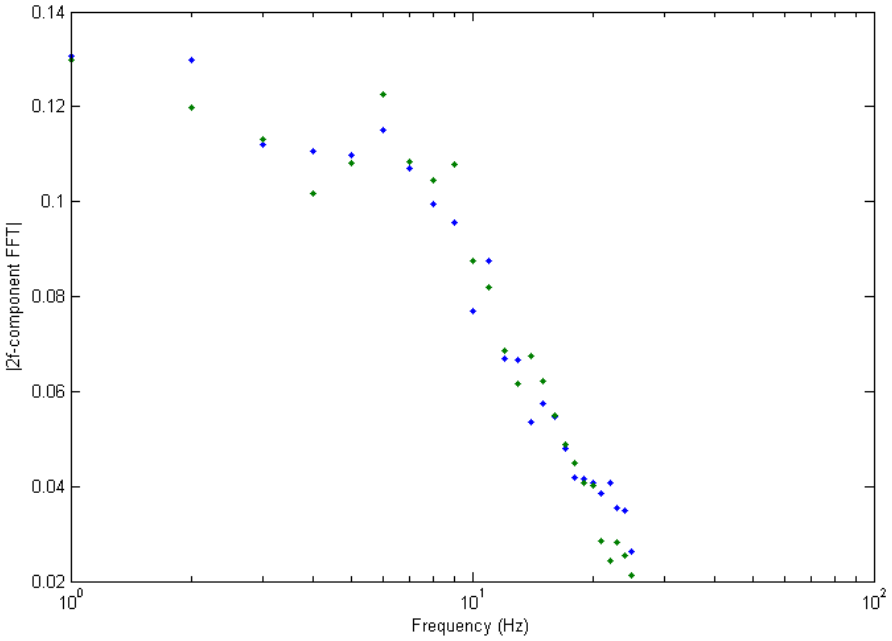

Figure D.3: The resulting graph of a measurement done using PBS as buffer, 100 times diluted beads, 0 pM target, a chaining field amplitude of 25 mT, a BSA concentration of 1% and 0.5% Tween® 20.

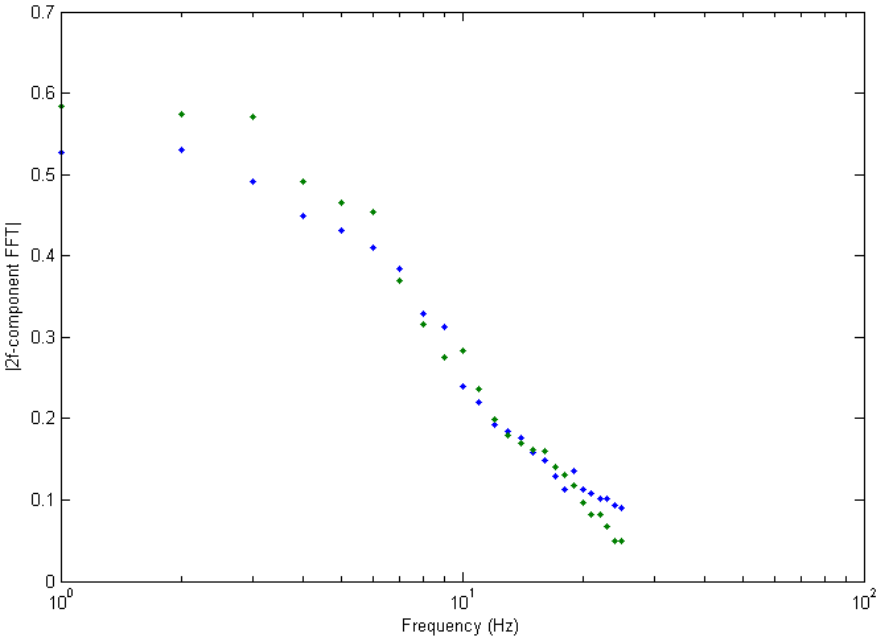

Figure D.4: The resulting graph of a measurement done using PBS as buffer, 100 times diluted beads, 50 pM target, a chaining field amplitude of 25 mT, a BSA concentration of 1% and 0.5% Tween® 20.

Appendix E: results of the variation of the chaining field amplitude using Tween®

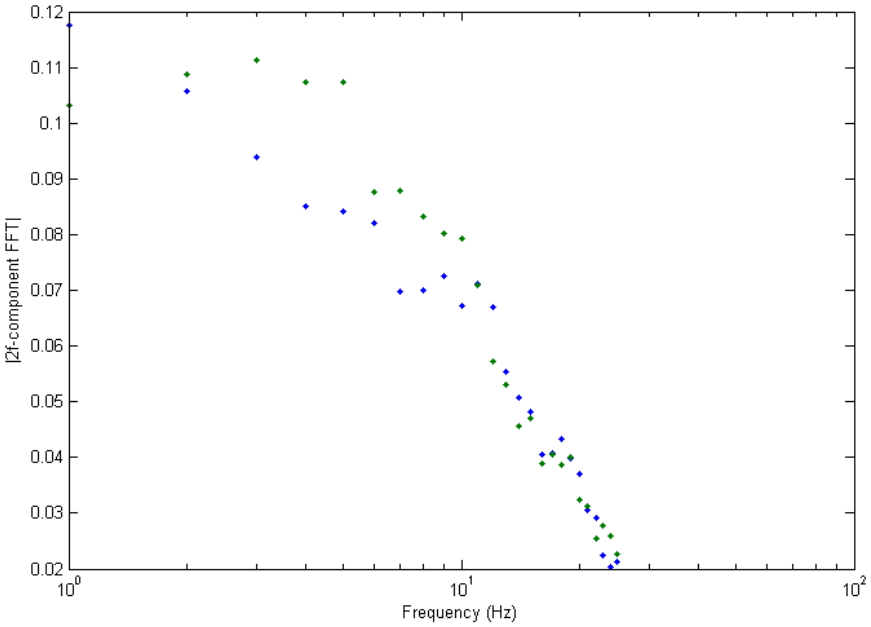

Figure E.1: The resulting graph of a measurement done using PBS as buffer, 100 times diluted beads, 0 pM target, a chaining field amplitude of 25 mT, a BSA concentration of 1% and 0.5% Tween® 20.

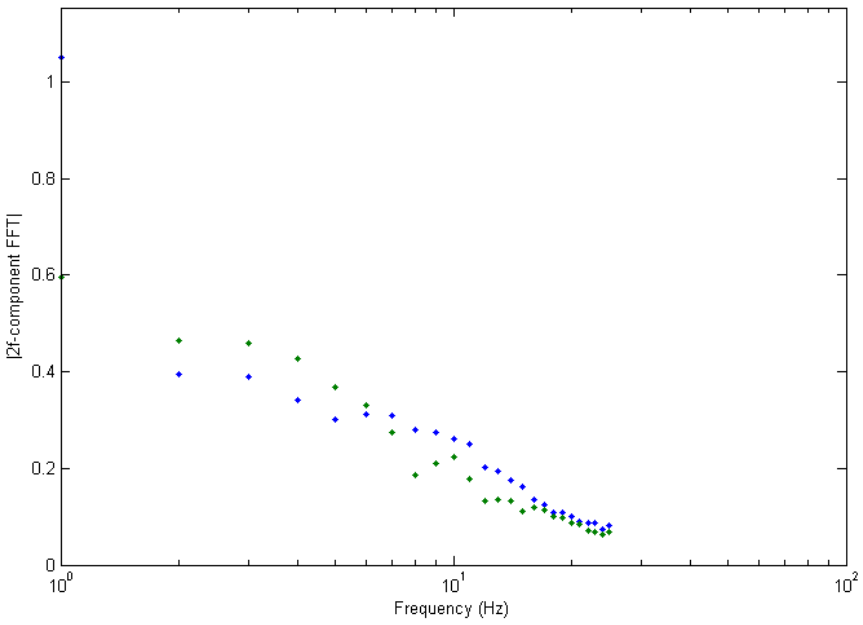

Figure E.2: The resulting graph of a measurement done using PBS as buffer, 100 times diluted beads, 50 pM target, a chaining field amplitude of 25 mT, a BSA concentration of 1% and 0.5% Tween® 20.

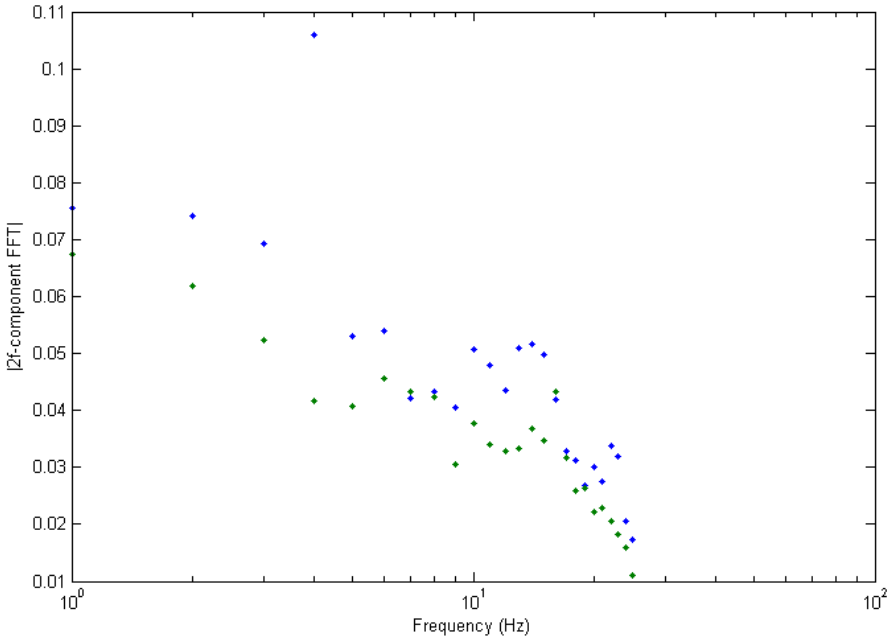

Figure E.3: The resulting graph of a measurement done using PBS as buffer, 100 times diluted beads, 0 pM target, a chaining field amplitude of 11.4 mT, a BSA concentration of 1% and 0.5% Tween® 20.

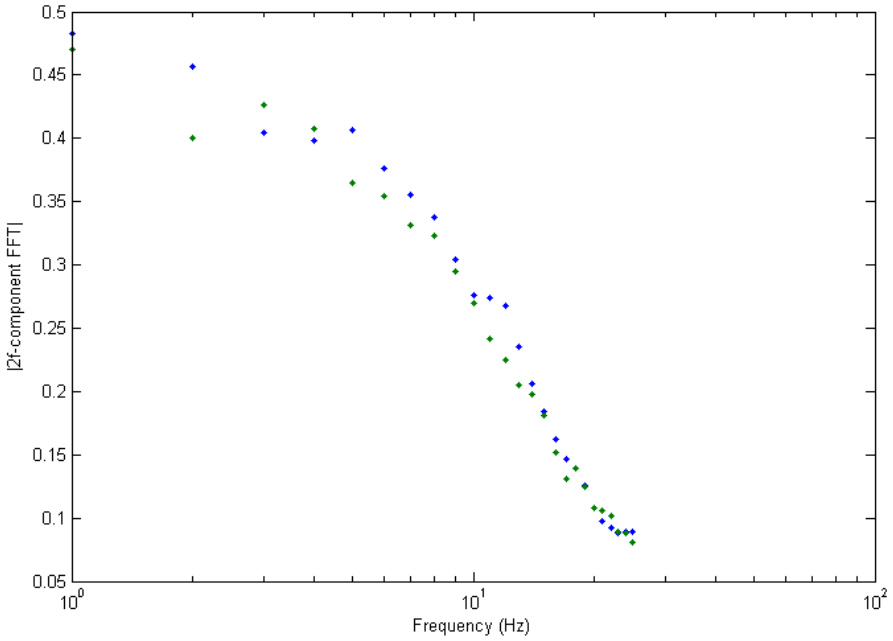

Figure E.4: The resulting graph of a measurement done using PBS as buffer, 100 times diluted beads, 50 pM target, a chaining field amplitude of 11.4 mT, a BSA concentration of 1% and 0.5% Tween® 20.

Appendix F: MATLAB scripts

MATLAB script for plotting the graphs

```
sample_freq = 10000;

%start_times = 600*sample_freq/1000)+sample_freq*[1:6:115 181:10:921]';
%Discard the first 0.6 seconds of each pulse.
%end_times = -400*(sample_freq/1000)+sample_freq*[3:6:117 186:10:926]';
%And discard the last 0.4 seconds of each pulse.
start_times = 180*sample_freq+sample_freq*(1:6:300)';
end_times = 180*sample_freq+sample_freq*(2:6:300)';

freqs(1:25) = 1:25;
freqs(26:50) = 1:25;
freqs = freqs(:);

sequence = [start_times end_times freqs];

folder = '    ';
datafiles = {' %Here comes the name of the file with photodiode data. '};

for I = 1:numel(datafiles)
    filename = [folder datafiles{i}];
    A = importdata(filename,'\t');
    Retstruct = analyse_PD_data(A,sequence,sample_freq);
    figure

semilogx(1:25,retstruct.chan_intensities(1,1:25,3),'.',1:25,retstruct.chan_
intensities(1,26:50,3),'.')
end
```

MATLAB script for importing and processing the photodiode data

```
function retstruct = analyse_PD_data(data,sequence,sample_freq)

%Time data and signal from all three photodiodes.
t = data(:,1);
chans = data(:,2:4); %0, 30 and 60 degrees PD.

%We know the frequency and time per pulse from the sequence variable:
IXs_start = sequence(:,1);
IXs_end = sequence(:,2);
Freqs = sequence(:,3);




%Check how many pulses there really are: If that is less than the
%number of indices, the sequence has not been completed (which is quite
%realistic as the last part is typically repeated a few times).
if IXs_end(end) > numel(t)
```

```
    for I = numel(IXs_end):-1:1
        if IXs_end(i) > numel(t)
           IXs_start(i) = [];
           IXs_end(i) = [];
           freqs(i) = [];
        end
    end
end

%The frequencies for all pulses are stored in freqs array, and the
%indices of data that need to be analyzed for each pulse are values of
%the form "IXs_start:IXs_end".

chan_intensities = zeros(3,numel(IXs_start),21);
chan_phases = zeros(3,numel(IXs_start),21);
    for i = 1:numel(IXs_start)
        start_time = IXs_start(i);
        end_time = IXs_end(i);
        freq = freqs(i);
        n_seconds = (end_time-start_time)/sample_freq;
        start_delay = 0.6+0.5/sample_freq;
        %Relates to the phase shift in the FFT.

        for PD_ID = 1:3
            %Spectrum of the signal of the photodiode
            freq_spectrum =
            fft(chans(start_time:end_time,PD_ID))/(end_time+1-start_time);
            chan_intensities(PD_ID,i,:) =
            abs(freq_spectrum(1:freq*n_seconds:(1+20*freq*n_seconds)));
            chan_intensities(PD_ID,i,2:21) =
            2*chan_intensities(PD_ID,i,2:21);
            chan_phases(PD_ID,i,:) =
            atan2(imag(freq_spectrum(1:freq*n_seconds:(1+20*freq*_seconds))
            ),real(freq_spectrum(1:freq*n_seconds:(1+20*freq*n_seconds))));
            chan_phases(PD_ID,i,:) = mod(chan_phases(PD_ID,i,:)-
            start_delay*2*pi*freq*reshape(0:20,1,1,21),2*pi);
        end
    end

    retstruct.freqs = freqs;
    retstruct.chan_intensities = chan_intensities;
    retstruct.chan_phases = chan_phases;

end
```